NOAA/NSIDC Climate Data Record of Passive Microwave Sea Ice Concentration, Version 4

USER GUIDE

How to Cite These Data

As a condition of using these data, you must include a citation:

Meier, W. N., F. Fetterer, A. K. Windnagel, and S. Stewart. 2021. *NOAA/NSIDC Climate Data Record of Passive Microwave Sea Ice Concentration, Version 4*. [Indicate subset used]. Boulder, Colorado USA. NSIDC: National Snow and Ice Data Center https://doi.org/10.7265/efmz-2t65. [Date Accessed].

FOR QUESTIONS ABOUT THESE DATA, CONTACT NSIDC@NSIDC.ORG

FOR CURRENT INFORMATION, VISIT https://nsidc.org/data/G02202/

TABLE OF CONTENTS

1 DATA DESCRIPTION

Notice: A near-real-time version of this data set also exists to fill the gap between the time that this data set is updated through to the present. The data set is called the *Near-Real-Time NOAA/NSIDC Climate Data Record of Passive Microwave Sea Ice Concentration* (G10016).

1.1 Summary

This data set provides passive-microwave-derived sea ice concentration (SIC) estimates that are produced in conformance with NOAA Climate Data Record (CDR) program criteria (NRC 2004). These criteria emphasize transparent and reproducible processing. The SIC CDR algorithm output is a rule-based combination of ice concentration estimates from two well-established SIC algorithms: the NASA Team (NT) algorithm (Cavalieri et al. 1984) and NASA Bootstrap (BT) algorithm (Comiso 1986). The SIC CDR algorithm blends the NT and BT output concentrations by selecting, for each grid cell, the higher concentration value. It capitalizes on the strengths of each contributing algorithm to produce ice concentration fields that should be more accurate than those from either algorithm alone. This statement is based on SIC CDR algorithm logic and the literature of NT and BT validation studies. Comprehensive validation of CDR ice concentration fields has not taken place. However, Meier et al. (2014) provide a detailed analysis of the spatial distributions of differences between the SIC CDR fields and ice concentration from NT and BT. They find that the CDR and BT fields are quite similar in both hemispheres. There are larger differences between CDR and NT, with the CDR (and BT) finding more ice overall. Trends in area and extent for all three products, computed over 1988-2007, have only small differences. This document summarizes important information about this data set including data file information and organization, spatial and temporal resolution, and data acquisition and processing. For full details on the algorithms, filters, interpolations, and error sources, see the Climate Algorithm Theoretical Basis Document (C-ATBD): Sea Ice Concentration (Meier et al., 2021).

The NT and BT algorithms run at NSIDC as part of SIC CDR processing. Separately, NASA Goddard Space Flight Center (GSFC) produces ice concentrations using the NT and BT algorithms that are distributed by the NSIDC DAAC as the following data sets: *Sea Ice Concentrations from Nimbus-7 SMMR and DMSP SSM/I-SSMIS Passive Microwave Data* (NSIDC-0051) and *Bootstrap Sea Ice Concentrations from Nimbus-7 SMMR and DMSP SSM/I-SSMIS* (NSIDC-0079), respectively. These products have some manual quality control applied and therefore do not meet CDR standards for reproducibility.

The SIC CDR begins in 1978 with NASA Nimbus-7 SMMR data with the variables `cdr_seaice_conc` for daily and `cdr_seaice_conc_monthly` for monthly. This data set is updated approximately every three to six months, after the input brightness temperature data (NSIDC-0001) become available. The closely related *Near-Real-Time NOAA/NSIDC Climate Data Record of Passive Microwave Sea Ice Concentration* fills the gap between the end date of this data set and present.

Daily and monthly resolution sea ice concentration values are provided in NetCDF files organized in two ways: 1) one file for each day of the year and one file for each month of the year for each hemisphere and 2) daily data aggregated into yearly files and monthly data aggregated into one period-of-record file for each hemisphere. Each file has a variable for the concentration product, as well as variables containing standard deviation, quality flags, and projection information. All data are on a 25 km x 25 km grid.

1.2 Parameters

The parameter of this data set is sea ice concentration which is the fraction of ocean area covered by sea ice. Sea ice concentration represents an areal coverage of sea ice. For a given grid cell, the parameter provides an estimate of the fractional amount of sea ice covering that cell, with the remainder of the area consisting of open ocean. Land areas are coded with a land mask value.

1.3 File Information

1.3.1 Format

These data are provided in NetCDF4 file format and are compliant with the Climate and Forecast (CF) Metadata Convention CF-1.6 (Eaton et al., 2010) and the Attribute Convention for Data Discovery (ACDD) 1.3.

The variables in both the daily and monthly NetCDF files are described in the sections 1.3.2.1 Daily File Variable Description and 1.3.2.2 Monthly File Variable Description, respectively.

1.3.2 File Contents

1.3.2.1 Daily File Variable Description

The daily NetCDF4 files contain the variables listed in Table 1, which provides a brief description of each. The sections below this table provide more detailed information.

Table 1. Daily Variables at a Glance. Click Variable Name for More Information.

Variable Name	Brief Description
cdr_seaice_conc	NOAA/NSIDC daily sea Ice concentration CDR
latitude	Latitude in degrees north of the projection grid centers (aggregated files only)
longitude	Latitude in degrees north of the projection grid centers (aggregated files only)
melt_onset_day_cdr_seaice_conc	The day of year on which melting sea ice was first detected in each grid cell for the daily NOAA/NSIDC SIC CDR (applies to the Northern Hemisphere only)
nsidc_bt_seaice_conc	NSIDC-processed Bootstrap daily sea ice concentrations
nsidc_nt_seaice_conc	NSIDC-processed NASA Team daily sea ice concentrations
projection	Projection information for the data
qa_of_cdr_seaice_conc	A number of different quality flags related to the daily NOAA/NSDIC SIC CDR.
spatial_interpolation_flag	Marks the grid cells that were spatially interpolated
stdev_of_cdr_seaice_conc	Standard deviation for the daily NOAA/NSIDC CDR sea ice concentration
temporal_interpolation_flag	Marks the grid cells that were temporally interpolated
time	Time in days since 1601-01-01 00:00:00
xgrid	X-offset in meters of the projection grid centers
ygrid	Y-offset in meters of the projection grid centers

cdr_seaice_conc

Description	NOAA/NSIDC CDR sea ice concentrations which is the fraction of ocean area covered by sea ice that span 25 October 1978 through most recent processing. This variable is merged from the NASA Team processed sea ice concentrations and Bootstrap processed sea ice concentrations using the SIC CDR Algorithm. For a description of the algorithm used to merge these, see section 2.3.3 SIC CDR Algorithm. See Table 2 for a list of all flag values.
Data Type	Byte array with dimensions [304, 448, 1] (North) and [316, 332, 1] (South), which are the xgrid, ygrid, and time, respectively. Note: The yearly aggregated daily files will have a time dimension of either 365 or 366 for the number of days in a year.
Valid Range	0 to 1. Note: Byte values are stored in the files from 0 to 100 but are presented by most, but not all, NetCDF readers as values ranging from 0 to 1 because of a scaling factor attribute (scale_factor) for this variable of .01 that is applied by most NetCDF readers. Flag values range from 251 to 255.
Fill Value	255
Units	Unitless

Table 2. Flag Values for Sea Ice Concentration Variables

Flag Name	Value
Northern Hemisphere pole hole (the region around the pole not imaged by the sensor)	251
Lakes	252
Coast/Land adjacent to ocean	253
Land	254
Missing/Fill	255

latitude

Description	Latitude in degrees north of the projection grid centers. This variable is only in the aggregated files.
Data Type	Float array with dimensions [304, 448] (North) and [316, 332] (South)
Valid Range	0.0 to 90.0 for northern hemisphere files, and -90.0 to 0.0 for southern hemisphere files.
Fill Value	-999.0
Units	Degrees north

longitude

Description	Longitude in degrees east of the projection grid centers. This variable is only in the aggregated files.
Data Type	Float array with dimensions [304, 448] (North) and [316, 332] (South)
Valid Range	-180.0 to 180.0
Fill Value	-999.0
Units	Degrees east

melt_onset_day_cdr_seaice_conc

Description	Contains the day of year on which melting sea ice was first detected in each grid cell. Once detected, the value is retained for the rest of the year. For example, if a grid cell started melting on day 73, the variable for the grid cell on that day will be 73, as will all subsequent days until the end of the year. The melt onset day is only calculated for the melt season: days 60 through 244, inclusive. Before melting is detected or if melt is never detected for that grid

	cell, the value will be -1 (missing / fill value). NOTE: This variable applies to Northern Hemisphere files only.
Data Type	Byte array with dimensions [304, 448, 1] (North), which are the xgrid, ygrid, and time, respectively. Note: The yearly aggregated daily files will have a time dimension of either 365 or 366 for the number of days in a year.
Valid Range	60 to 244
Fill Value	-1
Units	Unitless

nsidc_bt_seaice_conc

Description	NSIDC-processed Bootstrap daily sea ice concentrations from 25 October 1978 through most recent processing. For a list of flag values for this variable, see Table 2.
Data Type	Byte array with dimensions [304, 448, 1] (North) and [316, 332, 1] (South), which are the xgrid, ygrid, and time, respectively. Note: The yearly aggregated daily files will have a time dimension of either 365 or 366 for the number of days in a year.
Valid Range	0 to 1. Note: Byte values are actually stored in the files from 0 to 100 but are presented by most, but not all, NetCDF readers as values ranging from 0 to 1 because of a scaling factor attribute (scale_factor) for this variable of .01 that is applied by most NetCDF readers. Flag values range from 251 to 255.
Fill Value	255
Units	Unitless

nsidc_nt_seaice_conc

Description	NSIDC-processed NASA Team daily sea ice concentrations from 25 October 1978 through most recent processing. For a list of flag values for this variable, see Table 2.
Data Type	Byte array with dimensions [304, 448, 1] (North) and [316, 332, 1] (South), which are the xgrid, ygrid, and time, respectively. Note: The yearly aggregated daily files will have a time dimension of either 365 or 366 for the number of days in a year.
Valid Range	0 to 1. Note: Byte values are actually stored in the files from 0 to 100 but are presented by most, but not all, NetCDF readers as values ranging from 0 to 1 because of a scaling factor attribute (scale_factor) for this variable of .01 that is applied by most NetCDF readers. Flag values range from 251 to 255.
Fill Value	255
Units	Unitless

projection

Description	Provides details about the polar stereo projection information for the data. See section 1.4.2 Projection and Grid Description for more information.
Data Type	Char
Valid Range	N/A
Fill Value	N/A
Units	Meters

qa_of_cdr_seaice_conc

Description	A number of different quality flags related to the daily NOAA/NSDIC CDR sea ice concentration. See Table 3 for a list of the flags. Note: Grid cells that meet multiple conditions will have a value that is the sum of the values of each individual condition. For example, where the Bootstrap weather filter (`BT_weather_filter_applied`) and land spillover (`BT_land_spillover_filter_applied`) are applied, the flag value will be 5 (1 for BT weather plus 4 for BT land spillover).
Data Type	Byte array with dimensions [304, 448, 1] (North) and [316, 332, 1] (South), which are the xgrid, ygrid, and time, respectively. Note: The yearly aggregated daily files will have a time dimension of either 365 or 366 for the number of days in a year.
Valid Range	1 to 255
Fill Value	0
Units	Unitless

Table 3. Daily QA Flag Values

Condition	Flag Value	Label in NetCDF Variable	Description
BT weather filter applied	1	BT_weather_filter_applied	Indicates that the Bootstrap weather filter was applied to this grid cell. This means that sea ice concentration was set to zero (open ocean).
NT weather filter applied	2	NT_weather_filter_applied	Indicates that the NT weather filter was applied to this grid cell. This means that sea ice concentration was set to zero (open ocean).

Condition	Flag Value	Label in NetCDF Variable	Description
BT land spillover applied	4	BT_land_spillover_filter_applied	Indicates that the BT land-spillover correction was applied to this grid cell. This means that sea ice concentration was set to zero (open ocean).
NT land spillover applied	8	NT_land_spillover_filter_applied	Indicates that the NT land-spillover correction was applied to this grid cell. This means that the sea ice concentration was reduced by either 20%, 40%, or 60% depending on how far the grid cell is from the coast. If the value goes below zero, the concentration for that grid cell is set to zero.
Valid ice mask applied	16	valid_ice_mask_applied	Indicates that this grid cell has been designated as ocean (sea ice concentration set to zero) via an ocean mask or valid ice mask.
Spatially interpolation applied	32	spatial_interpolation_applied	Indicates that this grid cell was spatially interpolated. For more information, see the `spatial_interpolation_flag` variable.
Temporal interpolation applied	64	temporal_interpolation_applied	Indicates that this grid cell was temporally interpolated. For more information, see the `temporal_interpolation_flag` variable.

Condition	Flag Value	Label in NetCDF Variable	Description
Start of Melt Detected (Arctic only)	128	melt_start_detected	Indicates that the ice in this grid cell has shown evidence of starting to melt, so values may be less reliable. The melt onset test is used starting on day of year 60, around the time when the maximum sea ice extent is reached each year. Once a grid cell is flagged as melting, it remains so through the rest of the summer until day of year 244, roughly the time when extent reaches its minimum value. When the sea ice concentration is zero, the flag will be turned off. For the specific date that melt started, see the `melt_onset_day_cdr_seaice_conc` variable.

spatial_interpolation_flag

Description	Provides details on the grid cells that were spatially interpolated. Spatial interpolation occurs on the brightness temperature channels. See Table 4 for a list of the flag values and the Quality Control Procedures section of the C-ATBD (Meier et al., 2021) for details. If a grid cell was not spatially interpolated, then the value in this variable is set to zero for that grid cell.
Data Type	Byte array with dimensions [304, 448, 1] (North) and [316, 332, 1] (South), which are the xgrid, ygrid, and time, respectively. Note: The yearly aggregated daily files will have a time dimension of either 365 or 366 for the number of days in a year.
Valid Range	0 to 63
Fill Value	0
Units	Unitless

Table 4. Spatial interpolation flag values. A grid cell that satisfies more than one criteria will contain the sum of all applicable flag values.

Condition	Flag Value	Label in NetCDF Variable
19 GHz vertical brightness temperature spatially interpolated	1	19v_tb_value_interpolated
19 GHz horizontal brightness temperature spatially interpolated	2	19h_tb_value_interpolated
22 GHz vertical brightness temperature spatially interpolated	4	22v_tb_value_interpolated
37 GHz vertical brightness temperature spatially interpolated	8	37v_tb_value_interpolated
37 GHz horizontal brightness temperature spatially interpolated	16	37h_tb_value_interpolated
Pole hole spatially interpolated (Arctic only)	32	pole_hole_value_interpolated

stdev_of_cdr_seaice_conc

Description	Standard deviation for the daily NOAA/NSIDC CDR sea ice concentration. This value is the standard deviation of a given grid cell along with its eight surrounding grid cells (for nine values total) from both the NASA Team and Bootstrap data. This means that the standard deviation is computed using a total of 18 values: nine from the intermediate NISDC NASA Team data and nine from the intermediate NSIDC Bootstrap data. Grid cells with high standard deviations indicate values with lower confidence levels.
Data Type	Float array with dimensions [304, 448, 1] (North) and [316, 332, 1] (South), which are the xgrid, ygrid, and time, respectively. Note: The yearly aggregated daily files will have a time dimension of either 365 or 366 for the number of days in a year.
Valid Range	0.0 to 1.0
Fill Value	-1.0
Units	1

temporal_interpolation_flag

Description	Provides details on the grid cells that were temporally interpolated. Temporal interpolation is performed on the sea ice concentrations. See the Temporal Gap Filling Notes section of this document and the Sea Ice Concentration Temporal Interpolation section of the C-ATBD (Meier et al., 2021) for more details. The value for each flag is a 1- or 2-digit number indicating the data points used in the interpolation. For example, if the flag value is 24, then the missing grid cell was interpolated from sea ice concentration data from a grid cell from two days prior and four days in the future. If the value is 30, then the missing grid cell was filled with the sea ice concentration value from three days prior. If the value is one, then the missing grid cell was filled with the sea ice concentration value from one day in the future. If a grid cell was not temporally interpolated, then the value in this variable is set to zero for that grid cell.
Data Type	Byte array with dimensions [304, 448, 1] (North) and [316, 332, 1] (South), which are the xgrid, ygrid, and time, respectively. Note: The yearly aggregated daily files will have a time dimension of either 365 or 366 for the number of days in a year.
Valid Range	0 to 55
Fill Value	0
Units	Unitless

time

Description	Time in days since 1601-01-01 00:00:00.
Data Type	Float with a dimension of 1. Note: The yearly aggregated daily files will have a time dimension of either 365 or 366 for the number of days in a year.
Valid Range	N/A
Fill Value	N/A
Units	Days since 1601-01-01 00:00:00

xgrid

Description	X-offset in meters of the projection grid centers.
Data Type	Float array with dimension [304] (North) and [316] (South)
Valid Range	-3850000.0 to 3750000.0 (North) and -3950000.0 to 3950000.0 (South)
Fill Value	N/A
Units	Meters

ygrid

Description	Y-offset in meters of the projection grid centers.
Data Type	Float array with dimension [448] (North) and [332] (South)
Valid Range	-5350000.0 to 5850000.0 (North) and -3950000.0 to 4350000.0 (South)
Fill Value	N/A
Units	Meters

1.3.2.2 Monthly File Variable Description

The monthly NetCDF4 files contain the variables listed in Table 5, which provides a brief description of each. The sections below this table provide more detailed information.

Table 5. Monthly Variables at a Glance. Click Variable Name for More Information.

Variable Name	Brief Description
cdr_seaice_conc_monthly	NOAA/NSIDC monthly sea ice concentration CDR
latitude	Latitude in degrees north of the projection grid centers (aggregated files only)
longitude	Latitude in degrees north of the projection grid centers (aggregated files only)
melt_onset_day_cdr_seaice_conc_monthly	The day of year on which melting sea ice was first detected in each grid cell for the monthly NOAA/NSIDC SIC CDR. This applies to the Northern Hemisphere only.
nsidc_bt_seaice_conc_monthly	NSIDC-processed Bootstrap monthly sea ice concentrations
nsidc_nt_seaice_conc_monthly	NSIDC-processed NASA Team monthly sea ice concentrations
projection	Projection information for the data.
qa_of_cdr_seaice_conc_monthly	A number of different quality flags related to the monthly NOAA/NSDIC SIC CDR
stdev_of_cdr_seaice_conc_monthly	Standard deviation for the monthly NOAA/NSIDC CDR sea ice concentration
time	Time in days since 1601-01-01 00:00:00.
xgrid	X-offset in meters of the projection grid centers.
ygrid	Y-offset in meters of the projection grid centers.

cdr_seaice_conc_monthly

Description	The monthly average of the daily NSIDC-produced CDR sea ice concentrations (`cdr_seaice_conc`). For a description of the algorithm used to merge these, see section 2.3.3 SIC CDR Algorithm. See Table 2 for a list of all flag values.
Data Type	Byte array with dimensions [304, 448, 1] (North) and [316, 332, 1] (South), which are the xgrid, ygrid, and time, respectively. Note: The period-of-record aggregated monthly files will have a time dimension of the number of months since November 1978 through most recent processing.
Valid Range	0 to 1. Note: Byte values are actually stored in the files from 0 to 100 but are presented by most, but not all, NetCDF readers as values ranging from 0 to 1 because of a scaling factor attribute (scale_factor) for this variable of .01 that is applied by most NetCDF readers. Flag values range from 251 to 255.
Fill Value	255
Units	Unitless

latitude

Description	Latitude in degrees north of the projection grid centers. This variable is only in the aggregated files.
Data Type	Double array with dimensions [304, 448] (North) and [316, 332] (South)
Valid Range	0.0 to 90.0 for northern hemisphere files, and -90.0 to 0.0 for southern hemisphere files.
Fill Value	-999.0
Units	Degrees north

longitude

Description	Longitude in degrees east of the projection grid centers. This variable is only in the aggregated files.
Data Type	Double array with dimensions [304, 448] (North) and [316, 332] (South)
Valid Range	-180.0 to 180.0
Fill Value	-999.0
Units	Degrees east

melt_onset_day_cdr_seaice_conc_monthly

Description	Contains the day of year on which melting sea ice was first detected in each grid cell. Once detected, the value is retained for the rest of the year. For example, if a grid cell started melting on day 73, the variable for the grid cell on that day will be 73, as will all subsequent days until the end of the year. The melt onset day is only calculated for the melt season: days 60 through 244, inclusive. Before melting is detected or if melt is never detected for that grid cell, the value will be -1 (missing / fill value). Note: This variable applies to Northern Hemisphere files only.
Data Type	Integer array with dimensions [304, 448, 1] (North), which are the xgrid, ygrid, and time, respectively. Note: The period-of-record aggregated monthly files will have a time dimension of the number of months since November 1978 through most recent processing.
Valid Range	60 to 244
Fill Value	-1.0
Units	Unitless

nsidc_bt_seaice_conc_monthly

Description	NSIDC-processed Bootstrap monthly sea ice concentrations from 1978 through most recent processing. For a list of flag values for this variable, see Table 2.
Data Type	Byte array with dimensions [304, 448, 1] (North) and [316, 332, 1] (South), which are the xgrid, ygrid, and time, respectively. Note: The period-of-record aggregated monthly files will have a time dimension of the number of months since November 1978 through most recent processing.
Valid Range	0 to 1. Note: Byte values are actually stored in the files from 0 to 100 but are presented by most, but not all, NetCDF readers as values ranging from 0 to 1 because of a scaling factor attribute (scale_factor) for this variable of .01 that is applied by most NetCDF readers. Flag values range from 251 to 255.
Fill Value	255
Units	Unitless

nsidc_nt_seaice_conc_monthly

Description	NSIDC-processed NASA Team monthly sea ice concentrations from 1978 through most recent processing. For a list of flag values for this variable, see Table 2.
Data Type	Byte array with dimensions [304, 448, 1] (North) and [316, 332, 1] (South), which are the xgrid, ygrid, and time, respectively. Note: The period-of-record aggregated monthly files will have a time dimension of the number of months since November 1978 through most recent processing.
Valid Range	0 to 1. Note: Byte values are stored in the files from 0 to 100 but are presented by most, but not all, NetCDF readers as values ranging from 0 to 1 because of a scaling factor attribute (scale_factor) for this variable of .01 that is applied by most NetCDF readers. Flag values range from 251 to 255.
Fill Value	255
Units	Unitless

projection

Description	Provides details about the polar stereo projection information for the data. See section 1.4.2 Projection and Grid Description for more information.
Data Type	Char
Valid Range	N/A
Fill Value	N/A
Units	Meters

qa_of_cdr_seaice_conc_monthly

Description	A number of different quality flags related to the monthly NSDIC CDR sea ice concentration variable (`cdr_seaice_conc_monthly`). See Table 6 for a list of the monthly flags. Note 1: Grid cells that meet multiple conditions will have a value that is the sum of the values of each individual condition. For example, if spatial interpolation was performed and melt detected then the value will be 160 (32 + 128)
Data Type	Byte array with dimensions [304, 448, 1] (North) and [316, 332, 1] (South), which are the xgrid, ygrid, and time, respectively. Note: The period-of-record aggregated monthly files will have a time dimension of the number of months since November 1978 through most recent processing.
Valid Range	1 to 255
Fill Value	0
Units	Unitless

The QA flags listed in Table 6 include whether the average concentration exceeds 15%, which is commonly used to define the ice edge and can be used to easily quantify the total extent. Another flag indicates when average concentration exceeds 30%, which is a commonly used alternate ice edge definition. It may be desired to remove lower concentration ice that tends to have higher errors. Another flag indicates whether at least half the days have a concentration greater than 15%. This provides a monthly median extent, which may be a better representation of the monthly ice presence because an average conflates the spatial and temporal variation through the month. Additionally, there is a flag that indicates whether at least half the days have a concentration greater than 30%. This also provides a monthly median extent, but this higher percentage may leave out questionable or erroneous ice. There are flags to show if a cell was masked by the valid ice mask and whether spatial or temporal interpolation was performed. Finally, there is a flag to note whether melt was detected during the month. Since melt tends to bias concentrations lower, this flag gives a sense of whether melt has any effect on the monthly concentration estimate and whether it is having a dominating effect.

Table 6. Monthly QA Flag Values

Condition	Flag Value	Label in NetCDF Variable
Average concentration exceeds 15%	1	Average_concentration_exceeds_0.15
Average concentration exceeds 30%	2	Average_concentration_exceeds_0.30
At least half the days have sea ice conc > 15%	4	At_least_half_the_days_have_sea_ice_conc_exceeds_0.15
At least half the days have sea ice conc > 30%	8	At_least_half_the_days_have_sea_ice_conc_exceeds_0.30
Valid ice mask applied	16	Region_masked_by_ocean_climatology
At least one day during month has spatial interpolation	32	At_least_one_day_during_month_has_spatial_interpolation
At least one day during month has temporal interpolation	64	At_least_one_day_during_month_has_temporal_interpolation

Condition	Flag Value	Label in NetCDF Variable
Melt detected (at least one day of melt occurred during the month >= 1) (Arctic only)	128	At_least_one_day_during_month_has_melt_detected

stdev_of_cdr_seaice_conc_monthly

Description	Standard deviation for the monthly NOAA/NSIDC CDR sea ice concentration variable (`cdr_seaice_conc_monthly`). This value is the standard deviation of the concentration of all daily values for the month at that grid cell.
Data Type	Float array with dimensions [304, 448, 1] (North) and [316, 332, 1] (South), which are the xgrid, ygrid, and time, respectively. Note: The period-of-record aggregated monthly files will have a time dimension of the number of months since November 1978 through most recent processing.
Valid Range	0.0 to 1.0
Fill Value	-1.0
Units	Unitless

time

Description	Time in days since 1601-01-01 00:00:00.
Data Type	Float with a dimension of 1. Note: The period-of-record aggregated monthly files will have a time dimension of the number of months since November 1978 through most recent processing.
Valid Range	N/A
Fill Value	N/A
Units	Days since 1601-01-01 00:00:00

xgrid

Description	X-offset in meters of the projection grid centers.
Data Type	Float array with dimension [304] (North) and [316] (South)
Valid Range	-3850000.0 to 3750000.0 (North) and -3950000.0 to 3950000.0 (South)
Fill Value	N/A
Units	Meters

ygrid

Description	Y-offset in meters of the projection grid centers.
Data Type	Float array with dimension [448] (North) and [332] (South)
Valid Range	-5350000.0 to 5850000.0 (North) and -3950000.0 to 4350000.0 (South)
Fill Value	N/A
Units	Meters

1.3.2.3 Ancillary Files

Two ancillary files accompany this data set, one for the Northern Hemisphere and one for the Southern Hemisphere: G02202-cdr-ancillary-nh.nc and G02202-cdr-ancillary-sh.nc. These files contain the land mask, latitude, longitude, minimum concentration mask, pole hole masks, and valid ice masks used in processing the sea ice CDR. Table 7 describes the contents of these files.

Table 7. Ancillary file description

Variable	Description
crs	Coordinate reference system
landmask	Land mask with values 0: Ocean, 2: Lake, 253: Coast, 254: Land
latitude	Latitude in degrees at the center of the grid cell. Values range from 31.1 to 89.8 for the Northern Hemisphere and -39.4 to -89.8 for the Southern Hemisphere
longitude	Longitude in degrees at the center of the grid cell. Values range from 180 to -180
min_concentration	Minimum concentration mask with values 0: ocean far from land, 1: land, all others: minimum sea ice concentration in 10ths of K
month	Unit of time used to delineate the valid ice masks by month of the year.
polehole	Pole hole masks for SMMR, SSM/I, and SSMIS instruments. Values are bit masks and are additive: 0: No pole hole, 1: SMMR pole hole, 2: SSM/I pole hole, 4: SSMIS pole hole. For example, if the value of a grid cell is 7, this grid cell is inside all three pole hole masks.
valid_ice_mask	12 valid ice masks, one for each month of the year
x	X coordinate in meters
y	Y coordinate in meters

1.3.3 Directory Structure

The data files are organized on the HTTPS site into two main directories by hemisphere: `north` and `south`. The top-level directory also contains an `ancillary` directory that holds ancillary data files that may be useful when working with the sea ice CDR. Within each of the hemisphere directories, there are four sub-directories: `aggregate`, `checksums`, `daily`, and `monthly`. The `aggregate` directory contains the yearly aggregated daily files and the period-of-record aggregated monthly files. The `checksums` directory contains md5 checksums of the individual daily and monthly data files and the aggregated daily and monthly data files to ensure accuracy in data transfer. The `daily` directory contains the individual daily data files and is further sub-divided into directories labeled by the 4-digit year (YYYY) beginning with 1978; the daily files reside within their respective year directory. All individual monthly files reside directly in the `monthly` directory.

1.3.4 Naming Convention

The file naming convention for the daily and monthly files is listed below and described in Table 8:

Individual daily files: `seaice_conc_daily_hh_yyyymmdd_sat_vXXrXX.nc`
Yearly aggregated daily files: `seaice_conc_daily_hh_yyyy_vXXrXX.nc`
Individual monthly files: `seaice_conc_monthly_hh_yyyymm_sat_vXXrXX.nc`
Period-of-record aggregated monthly files:
`seaice_conc_monthly_hh_197811_yyyymm_vXXrXX.nc`

Where:

Table 8. File Naming Convention

Variable	Description
seaice_conc	Identifies files containing sea ice concentration data
daily	Identifies files containing daily sea ice concentration
monthly	Identifies files containing monthly sea ice concentration
hh	Hemisphere (nh: North, sh: South)
yyyy	4-digit year
mm	2-digit month
dd	2-digit day of month
sat	Satellite the data came from (n07: Nimbus 7, f08: DMSP F8, f11: DMSP F11, f13: DMSP F13,f17: DMSP F17)
vXXrXX	Version and revision number of the data file (v04r00: Version 4, Revision 0)
.nc	Identifies a NetCDF file
.nc.mnf	Identifies this as an md5 checksum file

1.4 Spatial Information

1.4.1 Coverage and Resolution

These data cover both the Northern and Southern polar regions at a 25 x 25 km grid cell size. Note: While resolution and grid cell size are often used interchangeably with regards to satellite data, there is an important difference. Resolution refers more properly to the instantaneous field of view (IFOV) of a particular sensor frequency. That is, resolution is the spot size on the ground that the sensor channel can resolve. The SSM/I channels used are the 19 GHz vertical, the 19 GHz horizontal, and the 37 GHz vertical. The IFOV of the 19 GHz SSM/I passive microwave channel is approximately 70 km x 45 km. See Table 2 in the C-ATBD (Meier et al., 2021) for a complete list of IFOVs by channel.

Since these data are gridded onto a 25 x 25 km grid and the IFOV of the sensor is coarser than this, the sensor is obtaining information from up to a 3 x 2 grid cell (~75 km x 45 km) region, but because a simple drop-in-the-bucket gridding method is used, that signature is placed in a single grid cell. This results in a spatial "smearing" across several grid cells. Also, some grid cells do not coincide with the center of the sensor footprint and are thus left as missing even though there is brightness temperature information available at that region. Higher frequency channels have finer resolution, but because the sea ice concentration algorithms use data from the 19 GHz channel, the sea ice concentration estimate is affected by the makeup of the surface over an area considerably larger than the nominal 25 km resolution.

The spatial coordinates for the Northern polar region are the following:

Northernmost Latitude: 31.10° N
Southernmost Latitude: 89.84° N
Easternmost Longitude: 180° E
Westernmost Longitude: 180° W

Note that for the Arctic, there is a region around the pole that is not imaged by the passive microwave sensors. This area is called the Arctic Pole Hole. Depending on the instrument used, the size of this area changes over time as the instrument changes. See Table 9 for these sizes.

With the release of Version 4, this area is now filled by spatial interpolation instead of being filled with missing values. Note, one cannot assume what the concentration is in the Arctic pole hole, especially in late Arctic summer and early autumn. Thus, we would advise caution in using the interpolated data in long-term trends or climatology analyses. See the C-ATBD (Meier et al., 2021) for more details.

Table 9. Arctic Pole Hole Size by Instrument

Instrument	Pole Hole Area (million km^2)	Pole Hole Radius (km)	Pole Hole Latitude
SMMR	1.19	611	84.5° N
SSM/I	0.31	311	87.2° N
SSMIS	0.029	94	89.18° N

The spatial coordinates for the Southern polar region are the following:

Southernmost Latitude: 89.84° S
Northernmost Latitude: 39.36° S
Westernmost Longitude: 180° W
Easternmost Longitude: 180° E

1.4.2 Projection and Grid Description

The sea ice concentration data are displayed in a polar stereographic projection. For more information on this projection, see the NSIDC Polar Stereographic Projections and Grids Web page. Note that the polar stereographic grid is not equal area; the latitude of true scale (tangent of the planar grid) is 70 degrees. Geolocation and grid details are given in Table 10 and Table 11.

Table 10. Geolocation Details

Geographic coordinate system	Unspecified datum based upon the Hughes 1980 ellipsoid
Projected coordinate system	Northern Hemisphere: NSIDC Sea Ice Polar Stereographic North Southern Hemisphere: NSIDC Sea Ice Polar Stereographic South
Longitude of true origin	Northern Hemisphere: -45° Southern Hemisphere: 0°
Latitude of true origin	Northern Hemisphere: 70° Southern Hemisphere: -70°
Scale factor at longitude of true origin	1
Datum	Not specified (based on Hughes 1980 ellipsoid)
Ellipsoid/spheroid	Hughes 1980
Units	meters
False easting	0°
False northing	0°
EPSG code	Northern Hemisphere: EPSG 3411 Southern Hemisphere: EPSG 3412

PROJ4 string	Northern Hemisphere: +proj=stere +lat_0=90 +lat_ts=70 +lon_0=-45 +k=1 +x_0=0 +y_0=0 +a=6378273 +b=6356889.449 +units=m +no_defs Southern Hemisphere: +proj=stere +lat_0=-90 +lat_ts=-70 +lon_0=0 +k=1 +x_0=0 +y_0=0 +a=6378273 +b=6356889.449 +units=m +no_defs

Table 11. Grid Details

Grid cell size	25 km x 25 km
Grid size (x, y pixel dimensions)	Northern Hemisphere: 448 x 304 Southern Hemisphere: 332 x 316
Geolocated lower left point in grid	Northern Hemisphere: 33.92° N, 279.26° E Southern Hemisphere: 41.45° S, 225.00 ° E
Nominal gridded resolution	25 km
Grid rotation	0
ulxmap – x-axis map coordinate of the center of the upper-left pixel	Northern Hemisphere: -3850000.0 Southern Hemisphere: -3950000.0
ulymap – y-axis map coordinate of the center of the upper-left pixel	Northern Hemisphere: 5850000.0 Southern Hemisphere: 4350000.0

1.5 Temporal Coverage and Resolution

The primary NOAA/NSIDC CDR sea ice concentrations (`cdr_seaice_conc` and `cdr_seaice_conc_monthly`) span 25 October 1978 to through most recent processing provided at both a daily resolution and a monthly averaged resolution (Table 12). For the monthly averaged data, at least 15 days of data must be available for a month for an average to be calculated. There is a gap in the data from 03 December 1987 through 12 January 1988 due to satellite issues during that time, so no daily or monthly data are available for that time period. There are additional gaps in the data due to corrupt or missing data that are noted in Table 13. Data files exist for these dates; however, they are filled with a missing data value of 255. In addition, dates of data that have partially corrupt data files are listed in Table 14 for reference, as they could cause issues in analyses of the time series because they contain values that look like sea ice concentration but that are clearly erroneous. Most of these data gaps occur during the SMMR era, which had some operational issues. See NSIDC Special Report 20 (Windnagel et al., 2021) for details on these corrupt and missing data. Many small gaps in the data (<10 days) are filled by temporal interpolation. See section 2.3.2.1 Temporal Gap Filling Notes for details.

In addition, a preliminary near-real-time version of this product is also available. The NRT SIC CDR is meant as an interim data set to fill the time period between updates of the final SIC CDR and to provide data up to the present. The NRT SIC CDR is preliminary and does not go through the same quality control measures that the final SIC CDR does, so it should be treated as such. You can access this interim product here: *Near-real-time NOAA/NSIDC Climate Data Record of Passive Microwave Sea Ice Concentration*.

Table 12. Time Period Each Instrument is Used in the SIC CDR

Platform and Instrument	Time Period
Nimbus-7 SMMR	25 October 1978 – 09 July 1987 Note: There are no data from 17 – 19 August 1984 due to satellite problems
DMSP-F8 SSM/I	10 July 1987 - 02 December 1991 Note: There are no data from 3 December 1987 through 12 January 1988 due to satellite problems.
DMSP-F11 SSM/I	03 December 1991 - 30 September 1995
DMSP-F13 SSM/I	01 October 1995 - 31 December 2007
DMSP-F17 SSMIS	01 January 2008 - most recent processing Note: There are no daily data for 24 March 2008, 25 March 2008, and 30 October 2008 due to satellite problems.

Table 13. Daily and monthly dates with no data due to corrupt or missing data

Arctic Daily: YYYY/MM/DD Monthly: Month Year	Antarctic Daily: YYYY/MM/DD Monthly: Month Year
1984/07/03 - 1984/08/04 July 1984	1984/08/12 - 1984/08/24 (Note: August 1984 is included but the average is calculated with less than half the days of the month available.)
1984/08/12 - 1984/08/24	1985/08/05 - 1985/08/09
1986/12/04 - 12/10/1986	1986/12/04 - 1986/12/10
1987/12/03 – 1988/01/13 December 1987 and January 1988	1987/12/03 – 1988/01/13 December 1987 and January 1988
1990/12/26 – 1990/12/27	2008/03/24 – 2008/03/25
2008/03/24 – /2008/03/25	

Table 14. Dates of partial SIC CDR fields due to corrupt or missing data
Note: Only dates where missing data affect sea ice concentration are noted here

Arctic (YYYY/MM/DD)	Antarctic (YYYY/MM/DD)
1979/06/07 - 1979/06/20	1982/08/04 - 1982/08/09
1986/03/28 - 1986/04/18	1984/08/25 - 1984/08/26
1990/12/25	1985/08/04
2008/03/26	1985/08/10 - 1985/08/11

	1986/03/30 - 1986/04/08
	1986/12/11 - 1986/12/12
	1990/12/26 – 1990/12/27
	2008/03/26

2 DATA ACQUISITION AND PROCESSING

2.1 Input Data

The input data for the sea ice CDR variables are described in Table 15.

Table 15. Variable Input Data

Satellite Era	Input Data Set Name
SMMR	*Nimbus-7 SMMR Polar Gridded Radiances and Sea Ice Concentrations, Version 1*
SSM/I and SSMIS	*DMSP SSM/I-SSMIS Daily Polar Gridded Brightness Temperatures, Version 5*

2.2 Acquisition

The input gridded brightness temperatures used for creating the daily NOAA/NSIDC CDR sea ice concentrations (`cdr_seaice_conc`) are archived at NSIDC in two data sets listed in Table 15. These SMMR gridded brightness temperatures were acquired from NASA and the SSM/I-SSMIS gridded brightness temperatures are produced by NSIDC from swath data obtained from Remote Sensing Systems (RSS). For a complete description of how the input data are processed, see the Data Acquisition and Processing sections in each data set user guide using the links in Table 15. The input data for the monthly CDR concentration (`cdr_seaice_conc_monthly`) are the daily sea ice concentration CDR data.

2.3 Derivation Techniques and Algorithms

2.3.1 Overview

NSIDC processes the input brightness temperatures (Table 15) into two different intermediate sea ice concentrations using two GSFC-developed algorithms: the NASA Team (NT) algorithm (Cavalieri et al., 1984) and the Bootstrap (BT) algorithm (Comiso, 1986). These intermediate NSIDC NT and BT sea ice concentrations are used in the NOAA/NSIDC SIC CDR algorithm described in further detail in the section 2.3.3 SIC CDR Algorithm.

The passive microwave channels employed for the sea ice concentration product are vertical (V) and horizontal (H) polarizations at 19 GHz (18.0 GHz for SMMR; 19.35 GHz for SSM/I and SSMIS), 22 GHz (V polarization only), and 37 GHz frequencies. Table 16 lists the channels used for each algorithm and the channels used for the weather filters. For a complete description of the weather filters, see the C-ATBD (Meier et al., 2021).

Table 16. NASA Team and Bootstrap Algorithm Channels

	NASA Team	Bootstrap
Algorithm Channels	19H, 19V, and 37V	37H, 37V, and 19V
Weather Filters	37V and 19V (SMMR, SSM/I, SSMIS) 22V and 19V (SSM/I, SSMIS)	37V and 19V (SMMR) 22V and 19V (SSM/I and SSMIS)

Since this data set uses multiple sensors over time, the sea ice algorithms are intercalibrated at the product (concentration) level by NASA GSFC. Thus, the brightness temperature source is less important because the intercalibration adjustment includes any necessary changes due to differences in brightness temperature across them. Both the NASA Team and Bootstrap algorithms employ varying tie-points to account for changes in sensors and spacecraft. These tie-point adjustments are derived from regressions of brightness temperatures during overlap periods. The adjustments are made at the product level by adjusting the algorithm coefficients so that the derived sea ice concentration fields are as consistent as possible.

The NASA Team approach uses sensor-specific hemispheric tie-points for each transition (Cavalieri et al., 1999; Cavalieri et al., 2011). Tie-points were originally derived for the SMMR sensor and subsequent transitions to the different SSM/I and SSMIS instruments adjusted the tie-points to be consistent with the original SMMR record. The Bootstrap algorithm uses daily varying hemispheric tie-points, derived via linear regression analysis on clusters of brightness temperature values of the relevant channels (Comiso, 2009; Comiso and Nishio, 2008). Also, in contrast to the NASA Team, Bootstrap tie-points for SMMR, SSM/I, and SSMIS are derived from matching fields from the AMSR-E sensor, which is newer and more accurate.

2.3.2 Automated Quality Control

Automated quality control measures are implemented independently on the intermediate NASA Team and Bootstrap outputs. Two weather filters, based on ratios of channels sensitive to enhanced emission over open water, are used to filter weather effects. Separate land-spillover corrections are used for each of the algorithms to filter out much of the error due to mixed land/ocean grid cells. Finally, to screen out errant retrievals of ice in regions where sea ice never occurs, valid ice masks are applied to the Northern Hemisphere and climatological ocean masks are applied to the Southern Hemisphere. In addition, temporal and spatial gap filling have been implemented for Version 4. For a complete description of the automated filters, masks, and gap filling, see the C-ATBD (Meier et al., 2021).

2.3.2.1 Temporal Gap Filling Notes

Gaps in the data can occur for many reasons from issues with the satellite, instrument, or ground stations collecting the data. Missing brightness temperature data can be in the form of no data at all for a day or more, entirely missing swath orbits, a few scans from a swath, or a few grid cells. To address these gaps and enhance the temporal and spatial completeness of the sea ice concentration CDR record, we have employed a temporal gap-filling approach described below along with guidelines for using the gap-filled data and an example of the effects of the method.

Two methods of temporal gap filling are performed on the data: two-sided and one-sided. The two-sided method, attempted first, linearly interpolates missing data with weighted values from up to five days on either side of the missing date. These days do not have to be evenly spaced because the method is searching for the closest days to the missing date possible. For example, a missing grid cell can be interpolated from corresponding grid cells one day in the past and one day in the future if those data exist; or the method may have to search further into the past or future to find values to interpolate with, such as two days in the past and four days in the future. Once a past and future value is found, the method stops searching for a value to interpolate with. The interpolation is weighted, whereby data closer to the missing date (e.g. 1 day away) are given more weight than data further away (e.g. 5 days away). If data are not available within five days before or after a date, the one-sided method is applied. This simpler approach fills a missing grid cell with a copy of the data value from the closest corresponding grid cell from up to three days on either side of the date.

We chose five days for the two-sided interpolation and three days for the one-sided interpolation based on experience, though these choices were somewhat arbitrary. If neither method can be applied, the grid cell is marked as missing.

A flag called temporal_interpolation_flag marks the grid cells that were temporally interpolated. This flag uses one- or two-digit numbers to indicate the known data points used in the interpolation. For two-sided gap filling, it is always a 2-digit number where the first digit indicates the number of days in the past, while the second digit indicates the number of days in the future from which the data point came from, with a max of five days in either direction. For example, a flag value of 24 indicates that the missing grid cell was linearly interpolated using sea ice concentration data from two days prior and four days in the future. In the two-sided method, the flag values range from 11 to 55 but exclude 10, 20, and 30. For the one-sided gap filing, where only one day is used, the value can be one or two digits with possible values of 1, 2, 3, 10, 20, and 30. Two-digit values indicate that data in the past were used, while single digit values indicate that data in the future were used. For example, a value of 30 indicates that data from three days in the past was copied.

Note: There is a bug in the one-sided interpolation whereby it is not looking for data into the future. Only the backward filling is being applied; so, values of 1, 2, or 3 can never occur. This bug will be fixed in a future version of the data product.

2.3.2.1.1 Guidelines for Using Temporally Interpolated Data

The temporal_interpolation_flag is provided as a way for users to screen for temporally gap-filled data. While the interpolation aims to provide the most complete fields possible, users can decide how much (if any) interpolation they wish to use based on the flag values. Here are some guidelines to consider when using the temporally interpolated data:

- The farther away from the day in question (i.e., the longer time period one is interpolating across) the less reliable the estimate.
- An asymmetry in the interpolation can also make the estimate less reliable (e.g. using data from 1 day in the past and 3 days in the future). Sea ice tends to grow linearly, so symmetrically weighted interpolation (i.e., same size gap before and after) typically yields reasonably good results. However, asymmetric, or especially one-directional, interpolation is less reliable.
- Another aspect is what spatial scale one is looking at. If one is looking at total extent or area for the entire Arctic or Antarctic, there is less sensitivity to interpolation because effects will average out. But if one is looking at a smaller region, then the interpolation could produce some odd-looking results.

2.3.2.1.2 Temporal Interpolation Example

Below is one example of how temporal gap filling works. In this example, two-sided and one-sided temporal gap filling work in conjunction. The example also illustrates the consequences of the bug in the one-sided gap filling noted above.

Due to an issue with the DMSP F17 satellite, there is no data at all for seven days from 19 March to 25 March 2008. The code attempts to fill this with temporal interpolation. Because this gap is larger than five days, a mix of the two-sided and one-sided interpolation is applied. The following bullets and Figure 1 describe what occurs for each grid cell and for each day during this gap:

- **March 18** is real data so the temporal_interpolation_flag is 0, i.e. no interpolation.
- **March 19** is a copy of March 18 because there is no data within five days into the future, so the one-sided gap filling technique is used. The temporal_interpolation_flag value is 10 indicating that the missing grid cells were filled with a copy of the data from one day prior.
- **March 20** is also a copy of March 18 because there is no data within five days into the future, so the one-sided gap filling technique is used. The temporal_interpolation_flag

value is 20, indicating that the missing grid cells were filled with the data from two days prior.

- **March 21** does have data within five days on either side, so it is gap filled using the two-sided method. The temporal_interpolation_flag values for this data are 35, so it is linearly interpolated with data from 3 days prior (March 18) and 5 days in the future (March 26).
- **March 22** does have data within five days on either side, so it is gap filled using the two-sided method. The temporal_interpolation_flag values for this data are 44, so it is linearly interpolated with data from 4 days prior (March 18) and 4 days in the future (March 26).
- **March 23** does have data within five days on either side, so it is gap filled using the two-sided method. The temporal_interpolation_flag values for this data are 53, so it is linearly interpolated with data from 5 days prior (March 18) and 3 days in the future (March 26).
- **March 24** is filled with missing but should be filled with a copy of data from March 26, since it's two days in the future, which is less than the three-day limit. This illustrates the bug in the one-sided method noted above.
- **March 25** is filled with missing but should be filled with a copy of data from March 26, since it's two days in the future, which is less than the three-day limit. This illustrates the bug in the one-sided method noted above.

Note that there is a jump from March 20 to March 21 since March 20 is a copy of March 18, but March 21 is linearly interpolated from data on March 18 and March 26.

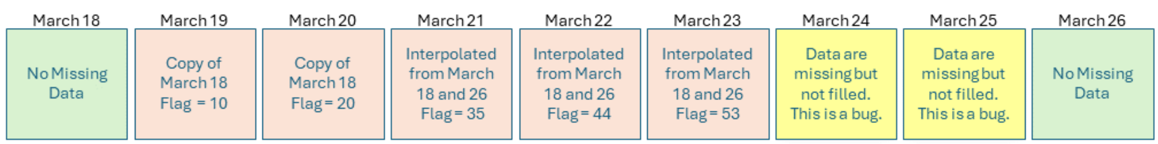

Figure 1. Temporal gap filling for the 7-day gap from 19 - 25 March 2008.

2.3.3 SIC CDR Algorithm

Different algorithms exist for computing sea ice concentration from brightness temperature data. The two widely used GSFC-developed NASA Team (Cavalieri et al., 1984) and Bootstrap (Comiso, 1986) algorithms are described in sections 2.3.4 and 2.3.5, respectively. Both algorithms have their own inherent advantages and limitations. For this SIC CDR data set, NSIDC processes the input brightness temperatures into two intermediate NASA Team and Bootstrap sea ice concentration fields following the way NASA produces their NASA Team and Bootstrap data sets with a few small differences. See the Theoretical Description section of the C-ATBD (Meier et al., 2021) for full details. The NASA-produced products are available from NSIDC as the *Sea Ice Concentrations from Nimbus-7 SMMR and DMSP SSM/I-SSMIS Passive Microwave Data* and the *Bootstrap Sea Ice Concentrations from Nimbus-7 SMMR and DMSP SSM/I-SSMIS*.

The NASA Team-derived sea ice concentrations are then merged with the Bootstrap-derived sea ice concentrations into a single ice concentration estimate. The SIC CDR algorithm steps are as follows:

- The sea ice concentrations estimated by the Bootstrap algorithm are analyzed first. Any grid cell with a concentration estimate of 10% or greater will be considered valid ice in the final product.
- For each grid cell that passes the Bootstrap threshold, the concentration value given by the NASA Team algorithm is compared with that given by the Bootstrap algorithm; whichever value is greater is selected as the CDR value.
- Any concentration values higher than 100% are set to 100%.

The resulting SIC CDR field has sea ice concentration values as low as 10% and as high as 100%.

Numerous studies, some noted below, have shown that passive microwave-based algorithms tend to underestimate true ice concentration. While both NASA Team and Bootstrap algorithms underestimate, the NASA Team algorithm tends to underestimate by a greater amount. The basis of the SIC CDR algorithm is that when compared, the algorithm estimate that is the highest concentration for a given grid cell is likely to be the more accurate estimate. The Bootstrap algorithm runs first because it generally does a better job at detecting ice in areas of low concentration and where the ice is thin.

The NASA Team algorithm, because it uses a ratio of brightness temperatures, tends to cancel out any physical temperature effects. The Bootstrap algorithm uses relationships between two brightness temperatures that are dependent on physical temperature. Thus, physical temperature changes can affect Bootstrap estimates. Errors occur primarily in regimes with very low temperatures: winter in the high Arctic and near the Antarctic coast (Comiso et al., 1997), where the Bootstrap algorithm can underestimate concentration and give a lower value than the NASA Team algorithm. During winter conditions with more moderate temperatures, NASA Team concentrations also tend to have more of a low bias (Kwok, 2002; Meier, 2005). During melt conditions, both algorithms tend to underestimate concentration; but the effect is more pronounced in the NASA Team algorithm (Comiso et al., 1997; Meier, 2005; Andersen et al., 2007).

While these characteristics of the algorithm are true in an overall general sense, ice conditions and algorithm performance can vary from grid cell to grid cell; and in some cases, this approach of choosing the larger value will result in an overestimation of concentration (Meier, 2005). However, using the higher concentration between the two algorithms will tend to reduce the overall underestimation of the SIC CDR estimate (Meier et al., 2014). For a more in-depth discussion on the reasoning behind the algorithm, see the Theoretical Description section of the C-ATBD (Meier et al., 2021).

2.3.4 NASA Team Algorithm

The NASA Team algorithm uses brightness temperatures from the 19 GHz V, 19 GHz H, and 37 GHz V channels. The methodology is based on two brightness temperature ratios, the polarization ratio (PR) of the 19 GHz V and H channels (Equation 1) and the spectral gradient ratio (GR) of the 19 GHz V and 37 GHz V channels (Equation 2).

$$PR(19) = [T_B(19V) - T_B(19H))]/[T_B(19V) + T_B(19H)]$$ **(Equation 1)**

$$GR(37V/19V) = [T_B(37V) - T_B(19V)]/[T_B(37V) + T_B(19V)]$$ **(Equation 2)**

Where:

Table 17. NASA Team Algorithm Variable Descriptions

Variable	Description
PR(19)	Polarization ratio of the 19 GHz vertical and horizontal channels
$T_B(19V)$	Brightness temperature at the 19 GHz vertical channel
$T_B(19H)$	Brightness temperature at the 19 GHz horizontal channel
GR(37V/19V)	Gradient ratio of the 37 GHz vertical channel and the 19 GHz vertical channel
$T_B(37V)$	Brightness temperature at the 37 GHz vertical channel

When PR and GR are plotted against each other, brightness temperature values tend to cluster in two locations, an open water (zero percent ice) point and a line representing 100 percent ice concentration, roughly forming a triangle. The concentration of a grid cell with a given GR and PR value is calculated by a linear interpolation between the open water point and the 100 percent line segment. See Figure 2.

For a detailed description of the NASA Team algorithm, please see the Descriptions of and Differences Between the NASA Team and Bootstrap Algorithms FAQ and the NASA Technical Memorandum 104647 (Cavalieri et al., 1997) that includes information about differences (for example, tie points) between the original algorithm and the revised NASA Team algorithm, and the NASA Team Algorithm section of the C-ATBD (Meier et al., 2021) for a table of tie-point values.

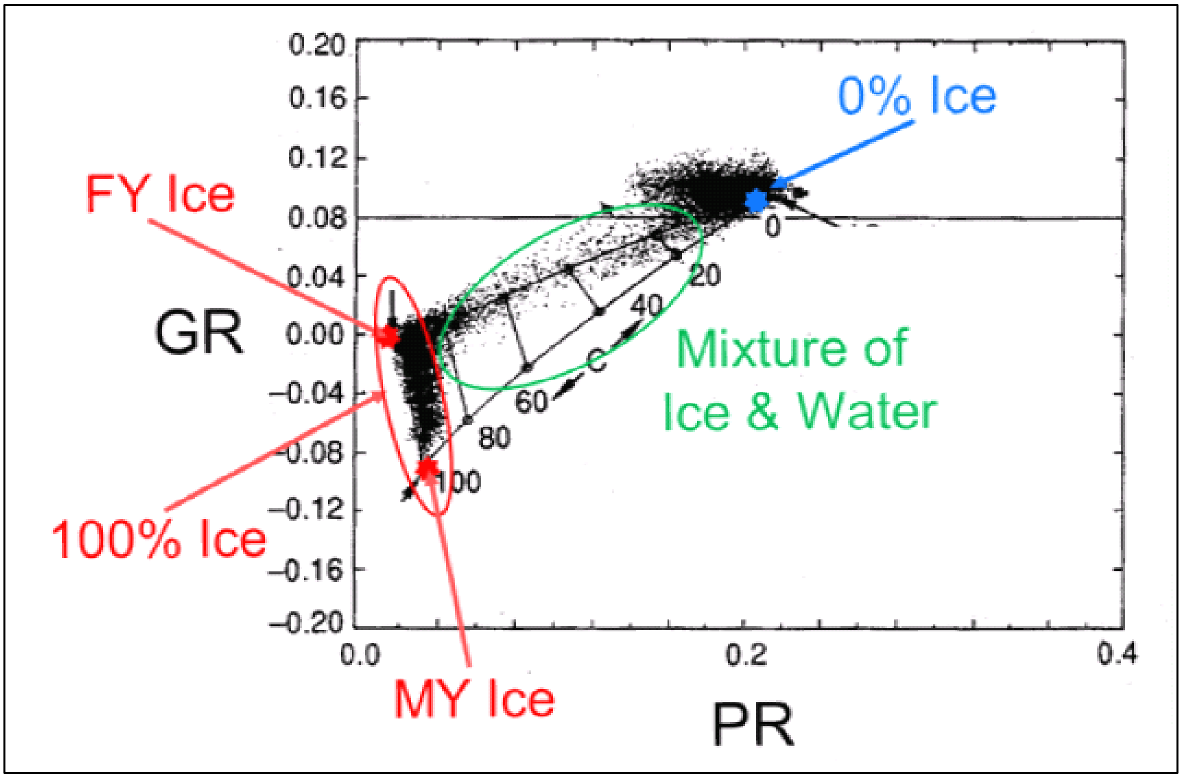

Figure 2. Sample plot of GR vs. PR with typical clustering of grid cell values (small dots) around the 0% ice (open water) point (blue star) and the 100% ice line (circled in red). Points with a mixture of ice and water (circled in green) fall between these two extremes. Adapted from Figure 10-2 of Steffen et al. (1992).

2.3.5 Bootstrap Algorithm

Like the NASA Team algorithm, the Bootstrap algorithm is empirically derived based on relationships of brightness temperatures at different channels. The Bootstrap method uses the fact that scatter plots of different sets of channels show distinct clusters that correspond to two pure surface types: 100 percent sea ice or open water.

Figure 3 shows a schematic of the general relationship between two channels. Points that fall along line segment AD represent 100 percent ice cover. Points that cluster around point O represent open water (zero percent ice). Concentration for a point B is determined by a linear interpolation along the distance from O to I where I is the intersection of segment OB and segment AD. This is described by Equation 3.

$C = (T_B - T_O)/(T_I - T_O)$ **(Equation 3)**

Where:

Table 18. Bootstrap Algorithm Variable Descriptions

Variable	Description
C	Sea ice concentration
T_B	Observed brightness temperature
T_O	Reference brightness temperatures for open water
T_I	Reference brightness temperatures for sea ice

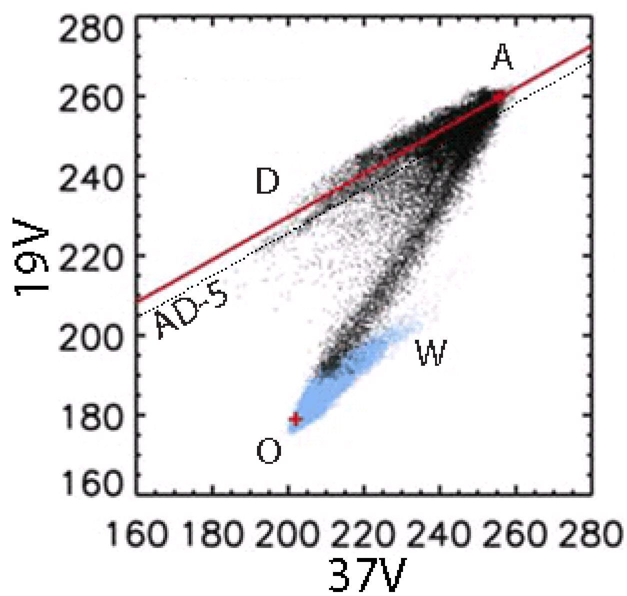

Figure 3. Example of the relationship of the 19V vs. 37V T_B (in Kelvin) used in the Bootstrap algorithm. Brightness temperatures typically cluster around the line segments AD (representing 100% sea ice) and OW (representing 100% open water). For points that fall below the AD-5 line (dotted line), Bootstrap uses T_B relationships for 37H vs. 37V. Adapted from Comiso and Nishio (2008).

The Bootstrap algorithm uses two such combinations, 37 GHz H versus 37 GHz V and 19 GHz V versus 37 GHz V, denoted as HV37 and V1937, respectively. Points that fall within 5 K of the AD segment in a HV37 plot, corresponding roughly to concentrations greater than 90 percent, use this approach. Points that fall below the AD-5 line, use the V1937 relationship to derive the concentration. Slope and offset values for line segment AD were originally derived for each hemisphere for different seasonal conditions (Table 2 in Comiso et al., 1997). However, a newer formulation, employed in this SIC CDR, was developed where slope and offsets are derived for each daily field based on the clustering within the daily brightness temperatures (Comiso and Nishio, 2008). For a detailed description of the Bootstrap algorithm, please see the Descriptions of and Differences Between the NASA Team and Bootstrap Algorithms FAQ.

2.4 Processing Steps

Below are the processing steps for both the daily and monthly data files. In addition, the source code is provided for transparency of the algorithm and processes used in creating the sea ice CDR. This source code is for reference only and is not intended to be portable to any computer system beyond that of the original SIC CDR producer's environment. You can access the code from the NOAA Climate Data Record Program's Operation CDR Web page under the Oceanic CDRs Sea Ice Concentration section.

2.4.1 Daily Files

The following are the general steps NSIDC uses to produce the daily NOAA/NSIDC CDR sea ice concentration product. See Figure 4 for a diagram of the data flow.

1. Obtain input brightness temperatures from the NSIDC *Nimbus-7 SMMR Polar Gridded Radiances and Sea Ice Concentrations* (NSIDC-0007) data set and the *DMSP SSM/I-SSMIS Daily Polar Gridded Brightness Temperatures* (NSIDC-0001) data set. See Table 16 for a list of channels used.
2. Spatially interpolate each brightness temperature channel. Fill the `spatial_interpolation_flag` variable. See the Quality Control Procedures section of the C-ATBD (Meier et al., 2021) for details.
3. Process the brightness temperatures into two intermediate sea ice concentration products using both the NASA Team and Bootstrap algorithms.
4. Apply weather filters, land-spillover corrections, and monthly valid ice masks.
5. Set some initial QA flags (`qa_of_cdr_seaice_conc`) based on the filters in step 4.
6. Temporally interpolate the intermediate NASA Team and Bootstrap sea ice concentrations. See the Quality Control Procedures section of the C-ATBD (Meier et al., 2021) for details.
7. For the Arctic, spatially interpolate the pole hole. See the Quality Control Procedures section of the C-ATBD (Meier et al., 2021) for details.
8. Merge the intermediate NSIDC NASA Team (`nsidc_nt_seaice_conc`) and Bootstrap (`nsidc_bt_seaice_conc`) data into the final SIC CDR using the SIC CDR algorithm and populate the `cdr_seaice_conc` variable. See section 2.3.3 SIC CDR Algorithm of this document for more information.
9. Apply a final weather filter and land-spillover correction and apply a day-of-year valid ice mask for the SMMR era to the sea ice concentration CDR.
10. Compute the CDR sea ice concentration standard deviation (`stdev_of_cdr_seaice_conc`) and the final QA flag values (`qa_of_cdr_seaice_conc`).
11. Calculate melt onset (`melt_onset_day_cdr_seaice_conc`) and add melt-indicator flag to the QA variable (`qa_of_cdr_seaice_conc`) via a post-processing step.
12. Populate the daily NetCDF variables and create the .nc files.

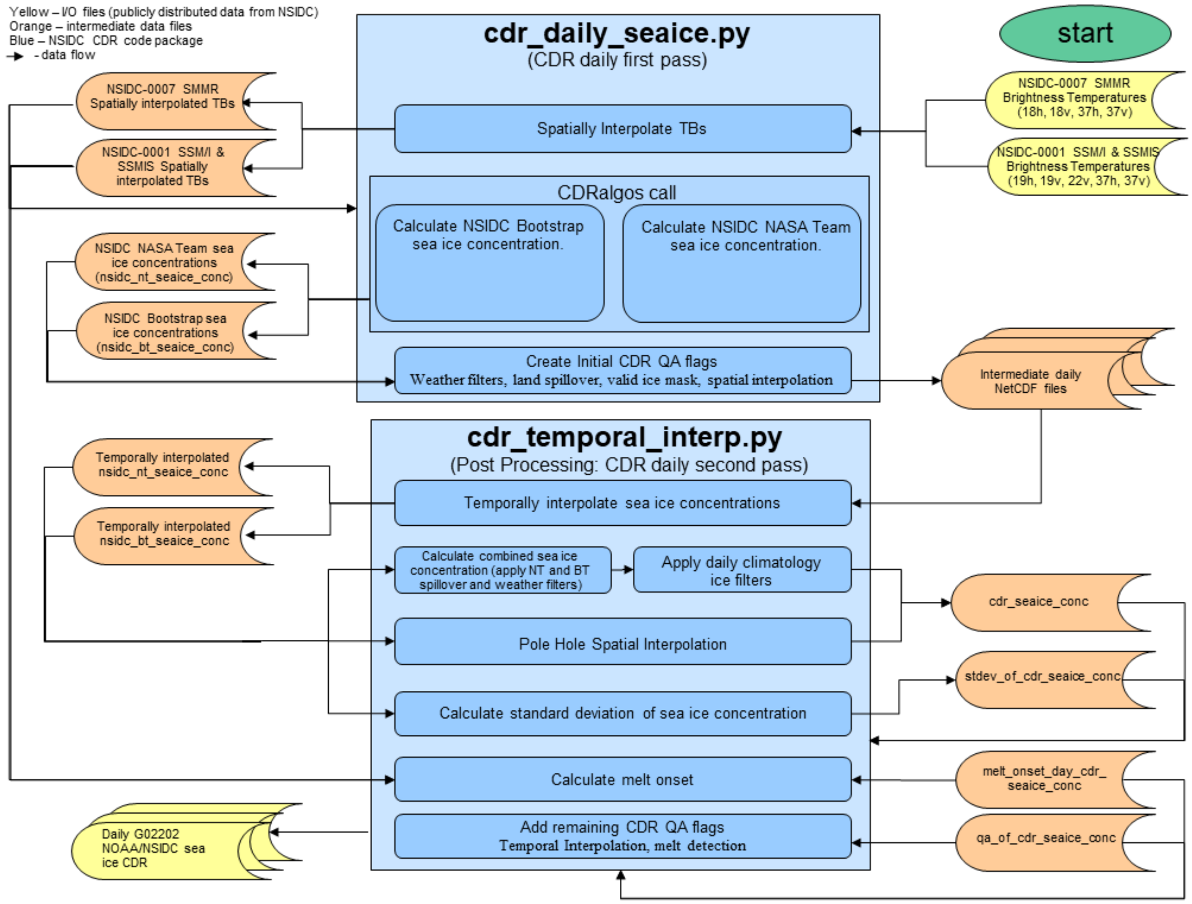

Figure 4. Flow of Data through the Daily SIC CDR Processing.

2.4.2 Monthly Files

The following are the general steps NSIDC uses to produce the monthly NOAA/NSIDC CDR sea ice concentration product. See Figure 5 for a diagram of the data flow.

1. Read the input daily NSIDC NASA Team and Bootstrap sea ice concentration data (`nsidc_nt_seaice_conc` and `nsidc_bt_seaice_conc`).
2. Compute the monthly mean concentration for each grid cell for a given month from the daily NASA Team and Bootstrap values.
3. Merge the monthly intermediate NSIDC NASA Team (`nsidc_nt_seaice_conc_monthly`) and Bootstrap (`nsidc_bt_seaice_conc_monthly`) data into the final SIC CDR using the SIC CDR algorithm and populate the `cdr_seaice_conc_monthly` variable. See section 2.3.3 SIC CDR Algorithm of this document for more information.
4. Compute the standard deviation and quality flags and fill those variables (`stdev_of_cdr_seaice_conc_monthly` and `qa_of_cdr_seaice_conc_monthly`).
5. Set melt onset day (value from the last day of the month) and fill the `melt_onset_day_cdr_seaice_conc_monthly` variable and add melt onset flag to the `qa_of_cdr_seaice_conc_monthly` variable.
6. Populate the monthly NetCDF variables and create the .nc files.

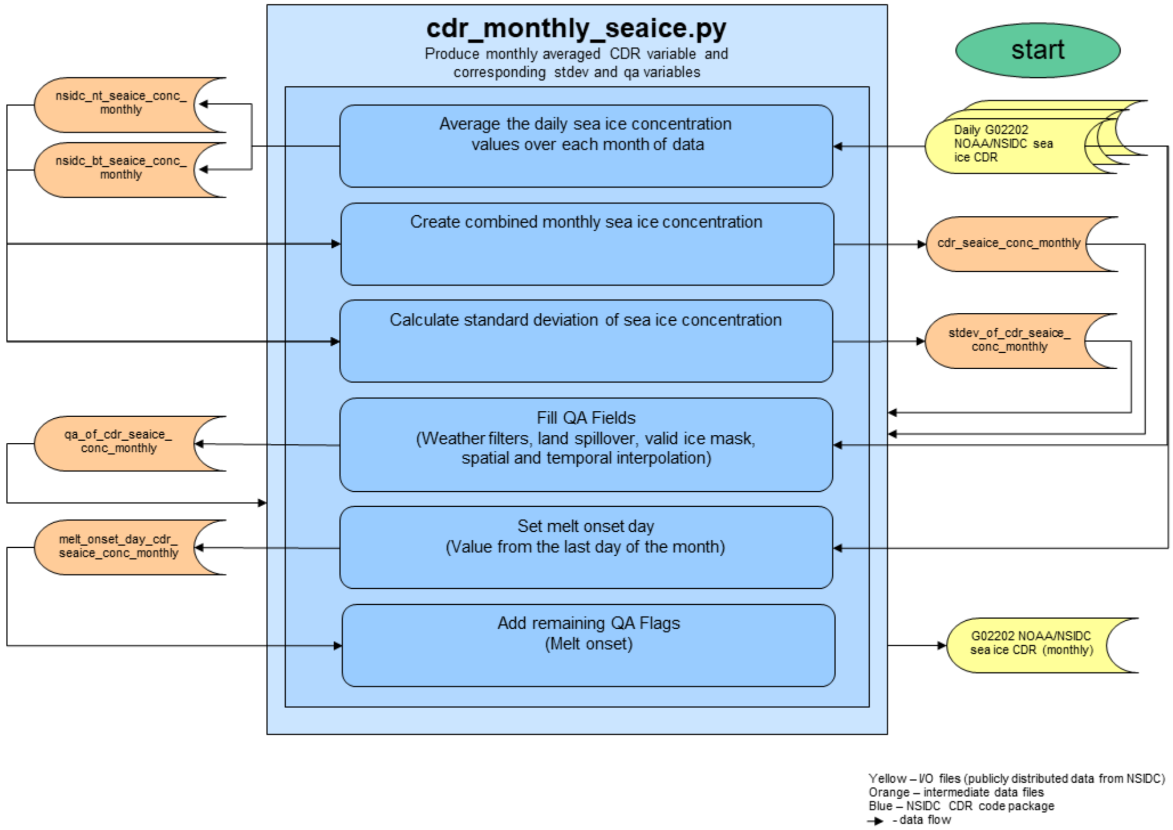

Figure 5. Flow of Data through the Monthly SIC CDR Processing.

2.5 Errors Sources

Several studies over the years have assessed sea ice concentration estimates from the NASA Team and Bootstrap algorithms. These assessments have typically used coincident airborne or satellite remote sensing data from optical, thermal, or radar sensors, generally at a higher spatial resolution than the SSM/I instrument but with only local or regional coverage. Several assessments indicate an accuracy of approximately five percent during mid-winter conditions away from the coast and the ice edge (Comiso et al., 1997; Ivanova et al., 2015; Kern et al., 2019; Meier et al., 2005; Andersen et al., 2007). Other assessments suggest concentration estimates are less accurate. Kwok (2002) found that passive microwave overestimates open water by three to five times in winter. Partington et al. (2003) found a difference with operational charts that was relatively low in the winter but rose to more than 20 percent in summer. In summer, due to surface melt and melt ponding, errors are higher (e.g., Kern et al., 2016; Kern et al., 2020).

Researchers can assess and improve a CDR by comparing it with operational products — real-time products that help ships cross the sea ice. Absolute error can be approximated via comparison to operational sea ice products, such as those produced by the U.S. National Ice Center (USNIC) or the Canadian Ice Service, but it is important to keep in mind that such products have an operational focus different from the climate focus of the SIC CDR, and the two are not expected to be consistent with each other. The documentation for the daily *Multi-Sensor Analyzed Sea Ice Extent* (MASIE), distributed by NSIDC in cooperation with USNIC, gives a summary of how satellite passive microwave SIC CDRs differ from operational products. An example of how the 15% contour in this SIC CDR product typically differs from the ide edge that analysts would find is given in Fetterer et al. (2021).

Errors can come from problems with the sensor, from weather effects, and from inadequacies in the algorithm. A satellite's orbit may drift over time, for example, which may degrade the data quality of an instrument. Most SSM/I instruments were used long past their designed lifetime expectancy. Atmospheric water vapor is a weather effect that can modulate the passive microwave signature of the surface, particularly at the 19 GHz frequency, causing ice concentration to be overestimated. The emissivity of sea water is generally stable, except under strong winds that cause waves to form. The emissivity of sea ice varies considerably depending on many factors including age, thickness, and surface roughness. When one considers that algorithms must arrive at a single number for ice concentration, taking into account the varying brightness temperatures of all the different surface types that may fill the footprints of the 19 GHz and 37 GHz channels, and that those footprints differ in size and shape across the instrument swath, one can appreciate the difficulty of the problem. Microwave Remote Sensing of Sea Ice, edited F. Carsey, provides a comprehensive overview of the subject (Carsey, 1992).

Another potential sensor error results from the transition between sensors on different platforms. The brightness temperature regression and tie-point adjustment corrects for this, though small artifacts remain (Cavalieri et al., 1999; Comiso and Nishio, 2008). Comparison of ice extent estimates from sensor overlap periods indicate that the adjustments yield agreements that are on the order of 0.05 percent or less and about 0.5 percent for sea ice area (Cavalieri et al., 1999; Cavalieri et al., 2011). Short overlap periods of early sensor transitions (SMMR to F8 and F8 to F11) may not account for the full seasonal variability (Meier and Khalsa, 2011b; Cavalieri et al., 2011) and differences may be higher in some cases. However, differences appear to be well below the sensitivity of the instrument, thus, providing confidence in the robustness of the intercalibrated algorithms through the time series.

When melt ponds form on the surface of ice floes in the summer, the ice concentration appears to decline when in fact the true concentration may not have changed (Fetterer and Untersteiner, 1998). Melt state is a surface effect that may in itself contain a climate trend, which could influence sea ice concentration trend estimates. This and other concentration error sources have been examined to some extent in Andersen et al. (2007), and their influence appears to be small compared to the estimated sea ice trends, but such effects should be kept in mind when using these data.

The NetCDF4 files contain a variable called `qa_of_cdr_seaice_conc` to help data users assess the quality of a given data value. For example, if the melt onset value is set, then there is higher error in the sea ice concentration value at that grid cell. Table 3 gives a list of the flags, their values, and their meaning. **Note**: Grid cells that meet multiple conditions will have a value that is the sum of the values of each individual condition.

For a more complete description of error sources and assessments, see the C-ATBD (Meier et al., 2021).

2.6 NSIDC-Processed NASA Team and Bootstrap Data Versus the GSFC-Produced Data

The NSIDC-processed NASA Team and Bootstrap sea ice concentration variables (`nsidc_nt_seaice_conc` and `nsidc_bt_seaice_conc`) are very similar to the GSFC-produced concentration available from NSIDC as the *Sea Ice Concentrations from Nimbus-7 SMMR and DMSP SSM/I-SSMIS Passive Microwave Data* and the *Bootstrap Sea Ice Concentrations from Nimbus-7 SMMR and DMSP SSM/I-SSMIS*. Although the differences are subtle, they are important.

The GSFC-produced concentrations include thorough quality control, including manual correction/replacement of bad values (for example, false ice due to weather effects over the ocean), and spatial or temporal interpolation to fill in missing values.

The NSIDC-processed concentrations are based on the same NASA Team and Bootstrap algorithms at Goddard but run in-house at NSIDC. There is automated spatial/temporal interpolation applied but there is no manual quality control.

The NSIDC-processed concentrations were created to meet the NOAA CDR Program criteria - most notably fully transparent and reproducible processing. The GSFC data do not meet this requirement because of the manual quality control aspect. However, this manual quality control likely results in a more accurate product but the automated quality control applied to the NSIDC concentrations is a good approximation of the manual inspection and is fully traceable.

For more details on the differences between the two different concentration products, see Meier et al. (2014) and Peng et al. (2013) which compare the two and show that the differences at the total extent/area level are mostly in the noise and there is very little difference in terms of trends.

2.7 Instrumentation

For the NOAA/NSIDC SIC CDR data, NSIDC uses brightness temperatures from the SMMR sensor on Nimbus-7 satellite, SSM/I sensors on the DMSP-F8, -F11, and -F13 platforms, and from the SSMIS sensor on DMSP-F17. See Table 19 for a description of orbital parameters of the different platforms. The rationale for using only these satellites was made to keep the equatorial crossing times as consistent as possible to minimize potential diurnal effects of data from sun-synchronous orbits of the DMSP satellites. For a list of the footprint size of each sensor by channel, see Table 2 in the C-ATBD (Meier et al., 2021).

Table 19. Comparison of Orbital Parameters

Parameter	Nimbus-7	DMSP-F8	DMSP-F11	DMSP-F13	DMSP-F17
Nominal Altitude*	955 km	860 km	830 km	850 km	850 km
Inclination Angle	99.1 degrees	98.8 degrees	98.8 degrees	98.8 degrees	98.8 degrees
Orbital Period	104 minutes	102 minutes	101 minutes	102 minutes	102 minutes
Ascending Node Equatorial Crossing (local time)	~ 12:00 p.m.	~ 6:00 a.m.	~ 5:00 p.m.	~ 5:43 p.m.	~5:31 p.m.
Instrument	SMMR	SSM/I	SSM/I	SSM/I	SSMIS
Algorithm Frequencies*	18.0, 37.0 GHz	19.4, 37.0 GHz	19.4, 37.0 GHz	19.4, 37.0 GHz	19.4, 37.0 GHz
Earth Incidence Angle*	50.2	53.1	52.8	53.4	53.1
3 dB Beam Width (degrees)*	1.6, 0.8	1.9, 1.1	1.9, 1.1	1.9, 1.1	1.9, 0.4

*Indicates sensor and spacecraft orbital characteristics of the three sensors used in generating the sea ice concentrations.

3 SOFTWARE AND TOOLS

3.1 NetCDF Description

The NetCDF format is a self-describing file format for array-oriented data. For more information on this file format see the NSIDC What is NetCDF? web page and the links therein.

3.2 STAC Catalog

We provide a SpatioTemporal Asset Catalog (STAC) to improve the accessibility and discoverability of the SIC CDR. A STAC catalog provides special metadata about the collection that provides a standardized way to expose the spatio-temporal data and allows it to be more easily worked with, indexed, and discovered. In this section, we describe the catalog and provide examples of how to utilize it.

A STAC catalog uses a JSON schema to describe the data via different STAC specifications. For this STAC, we use the *Collection* and *Item* specifications. The *Collection* specification is used to describe a group of related *Items* using a set of common metadata fields. In this case, the *Collection* is the entire SIC CDR data product. The *Item* specification is used to describe each asset of the *Collection*. In this case, each individual SIC CDR NetCDF file. Thes two specifications provide product-level (*Collection*) and file-level (*Item*) metadata for the data set.

This catalog begins with a JSON file that defines the *Collection* in a file called `collection.json`. Each *Item* represents a single spatio-temporal asset of the catalog, and each is described in its own JSON file. For the SIC CDR, there is one *Item* file for each daily and monthly aggregated NetCDF file for the northern and southern hemispheres. The *Item* JSON files have the following file naming conventions:

Daily aggregated: seaice_conc_daily_[Xh]_[YYYY]_v04r00.json

Monthly aggregated: seaice_conc_monthly_[Xh]_197811_[YYYYMM]_v04r00.json

Where:

Variable	Description
Xh	Hemisphere (nh = northern hemisphere, sh = southern hemisphere).
YYYY	For the daily aggregated files, this is the year of the data within the files.
YYYYMM	For the monthly aggregated file, this is the year and month of the end date of the data in the file. Data span the entire time series in the monthly aggregated files from November 1978 through most recent processing.

This STAC Catalog is located here: https://noaadata.apps.nsidc.org/NOAA/G02202_V4/stac/.

Examples of how to utilize the STAC catalog using Python can be found on NSIDC’s GitHub repository in the Sea Ice CDR Learning Notebooks tutorial at https://github.com/nsidc/seaice-cdr-learning-notebook.

4 VERSION HISTORY

Table 20. Version History

Version	Release Date	Description of Changes
v04r00	June 2021	Release of Version 4 Revision 0 1. Added SMMR data to the period of record so that the daily SIC CDR sea ice variable now spans 25 October 1978 through to the most recent processing, and the monthly SIC CDR variable will span from November 1978 through to the most recent processing. 2. Added NSIDC-produced daily and monthly NASA Team (NT) and NASA Bootstrap (BT) variables: • nsidc_nt_seaice_conc • nsidc_bt_seaice_conc • nsidc_nt_seaice_conc_monthly • nsidc_bt_seaice_conc_monthly. 3. Gap filling implemented using spatial and temporal interpolation. Two new flag variables (spatial_interpolation_flag and temporal_interpolation_flag) indicate when interpolation has been done. 4. Arctic pole hole filled by spatial interpolation. 5. NSIDC's BT algorithm has been updated to use Goddard's BT version 3.1 algorithm, the current version for the BT product. 6. Updated the NASA Team GR3719 weather filter threshold from 0.053 to 0.057 for the Southern Hemisphere F17 and F18 SSMIS instruments and updated it from 0.07 to 0.076 for the Southern Hemisphere SMMR instrument. 7. In SIC CDR V4, both the NT and BT weather and land spillover filters were applied where as in V3, only the BT filters were applied. 8. The following variables have been renamed: • seaice_conc_cdr → cdr_seaice_conc • melt_onset_day_seaice_conc_cdr → melt_onset_day_cdr_seaice_conc • stdev_of_seaice_conc_cdr → stdev_of_cdr_seaice_conc • qa_of_seaice_conc_cdr → qa_of_cdr_seaice_conc • seaice_conc_monthly_cdr → cdr_seaice_conc_monthly • melt_onset_day_seaice_conc_cdr_monthly → melt_onset_day_cdr_seaice_conc_monthly • stdev_of_seaice_conc_monthly_cdr → stdev_of_cdr_seaice_conc_monthly • qa_of_seaice_conc_monthly_cdr → qa_of_cdr_seaice_conc_monthly 9. Removed the following Goddard-produced variables: • goddard_merged_seaice_conc • goddard_nt_seaice_conc • goddard_bt_seaice_conc • goddard_merged_seaice_conc_monthly • goddard_nt_seaice_conc_monthly • goddard_bt_seaice_conc_monthly 10. In addition to the individual daily and monthly NetCDF files, yearly aggregated files containing daily data and period-of-record aggregated files containing monthly data are available for download. 11. Land masks merged into one composite land mask.
v03r01	October 2018	The data have been processed through 31 December 2017. The input data to the Goddard BT variables have been versioned up from v3.0 to v3.1 for 2017 data onward. This change does not affect the sea ice concentration CDR data variables.

Version	Release Date	Description of Changes
v03r01	December 2017	Release of Version 3 Revision 1 Incorporated a new version of the input data product, Bootstrap Sea Ice Concentrations from Nimbus-7 SMMR and DMSP SSM/I-SSMIS, Version 3. With this new version of the Bootstrap data, the data providers made some modifications to the Bootstrap algorithm. See the Bootstrap documentation for a description of these modifications. Note that the sea ice CDR product has not been updated to incorporate these modification, so the Bootstrap algorithm used to produce the SIC CDR and the one used to produce the Bootstrap data product are currently inconsistent. NSIDC will be address this inconsistency in a future version of the SIC CDR product. In addition, the Bootstrap data providers chose to remove a section of data from 02 December 1987 through 13 January 1988 that is of poor quality due to issues with the satellite during that time period. This time period had already been removed by the data providers of the NASA team data product, Sea Ice Concentrations from Nimbus-7 SMMR and DMSP SSM/I-SSMIS Passive Microwave Data. However, NSIDC had continued to provide data files for this time period because Bootstrap data were still being provided. Because the Bootstrap data providers have decided to remove this time period from their product, NSIDC has removed all daily and monthly data files for this time period for the sea ice CDR, as well, since there is no data for that time period. Further, the Bootstrap data providers also chose to change the start date of their data set from 26 October 1978 to 01 November 1978. Since there are no longer bootstrap data for October 1978, the sea ice CDR data set now also begins 01 November 1978. Fixed a bug in the code that was causing some sections of the time series to not produce output files. The data have been processed through 28 February 2017. Updated the data that use the SSMIS instrument (01 January 2008 to present) to also use the SSMIS pole hole mask. In previous versions, the larger SSM/I pole hole mask was being used for these data, which was cutting out a section of valid data.
v03r00	August 2017	Release of Version 3 Revision 0 The mask to remove spurious ice was updated for the Northern Hemisphere from the NH climatology ocean masks to the Polar Stereographic Valid Ice Masks Derived from National Ice Center Monthly Sea Ice Climatologies. See the C-ATBD (Meier et al., 2021) for complete details on the use of these masks.
v02r00	August 2015	The production code was refactored and modularized to improve its internal structure, however, the data were not changed or affected by this update to the code. Data from 1978 through 2013 were processed with the non-modularized version of the code, and 2014 data were processed with the new modularized code.
v02r00	June 2013	Release of Version 2 Two new variables were added to the data set NetCDF4 files: • `melt_onset_day_cdr_seaice_conc` • `melt_onset_day_cdr_seaice_conc_monthly` Calculation of `melt_start_detected` flag in the `qa_of_seaice_conc_cdr` variable was updated.

Version	Release Date	Description of Changes
v01r00	September 2011	Initial release of sea ice CDR.

5 RELATED DATA SETS

- *Near-real-time NOAA/NSIDC Climate Data Record of Passive Microwave Sea Ice Concentration*
- *DMSP SSM/I-SSMIS Daily Polar Gridded Brightness Temperatures*
- *Sea Ice Concentrations from Nimbus-7 SMMR and DMSP SSM/I Passive Microwave Data*
- *Bootstrap Sea Ice Concentrations from Nimbus-7 SMMR and DMSP SSM/I*
- *Multi-sensor Analyzed Sea Ice Extent (MASIE)*
- *Sea Ice Index*
- *Gridded Monthly Sea Ice Extent and Concentration, 1850 Onward*
- *AMSR-E/Aqua Daily L3 12.5 km Brightness Temperatures, Sea Ice Concentration, & Snow Depth Polar Grids*
- *AMSR-E/Aqua Daily L3 25 km Brightness Temperatures & Sea Ice Concentration Polar Grids*

6 RELATED WEBSITES

- NOAA's National Centers for Environmental Information (NCEI) Climate Data Record (CDR) program
- EUMETSAT Ocean & Sea Ice Satellite Application Facility
- Sea Ice Concentration: NOAA/NSIDC Climate Data Record: Provides an overview of the data product's strengths and weaknesses (Meier and NCAR, 2014).

7 CONTACTS AND ACKNOWLEDGMENTS

Walt Meier (PI)

Florence Fetterer (Co-I)

National Snow and Ice Data Center (NSIDC)

Boulder, Colorado USA

The development of this product was supported in part by a grant NA07OAR4310056 from the NOAA NCEI Climate Data Record Program. Production of original NASA Team and Bootstrap algorithm estimates supported by the NASA Polar Distributed Active Archive Center. The sea ice concentration algorithms were developed by Donald J. Cavalieri, Josefino C. Comiso, Claire L. Parkinson, and others at the NASA Goddard Space Flight Center in Greenbelt, Maryland, USA. It is maintained at NSIDC with support from the NOAA National Centers for Environmental Information.

8 REFERENCES

Andersen, S., Tonboe, R., Kaleschke, L., Heygster, G., and Pedersen, L. T. (2007). Intercomparison of Passive Microwave Sea Ice Concentration Retrievals over the High-Concentration Arctic Sea Ice. *J. Geophys. Res.*, 112(C08004). doi:10.1029/2006JC003543.

Belchansky, G. I., and D. C. Douglas. (2002). Seasonal Comparisons of Sea Ice Concentration Estimates Derived from SSM/I, OKEAN, and RADARSAT Data. *Rem. Sens. Environ.*, 81: 67-81.

Carsey, F. D. (Ed.). (1992). Microwave Remote Sensing of Sea Ice. *American Geophysical Union*, 462 pp.

Cavalieri, D., C. Parkinson, N. DiGirolamo, A. Ivanov (2011). Intersensor calibration between F13 SSM/I and F17 SSMIS for global sea ice data records. *IEEE Geosci. Remote Sens. Lett*., 9(2), 233-236, doi:10.1109/LGRS.2011.2166754.

Cavalieri, D., C. Parkinson, P. Gloersen, J. Comiso, and H. J. Zwally (1999). Deriving Long-term Time Series of Sea Ice Cover from Satellite Passive-microwave Multisensor Data Sets. *J. of Geophys. Res.*, 104(C7):15,803-15,814.

Cavalieri, D. J., C. L. Parkinson. (1997). Arctic and Antarctic Sea Ice Concentrations from Multichannel Passive-Microwave Satellite Data Sets: October 1978 - September 1995 - User's Guide. *NASA Technical Memorandum* 104647. NASA Goddard Space Flight Center, Greenbelt, Maryland.

Cavalieri, D. J., P. Gloersen, and W. J. Campbell. (1984). Determination of Sea Ice Parameters with the NIMBUS-7 SMMR. *J. Geophys. Res*., 89(D4): 5355-5369.

Comiso, J.C., R.A. Gersten, L.V. Stock, J. Turner, G.J. Perez, and K. Cho. (2017). Positive Trend in the Antarctic Sea Ice Cover and Associated Changes in Surface Temperature. *J. Climate*, 30, 2251–2267. doi: 10.1175/JCLI-D-16-0408.1.

Comiso, J. C. (2009). Enhanced Sea Ice Concentrations and Ice Extents from AMSR-E Data. *J. Rem. Sens. of Japan,* 29(1):199-215.

Comiso, J. C., and F. Nishio. (2008). Trends in the Sea Ice Cover Using Enhanced and Compatible AMSR-E, SSM/I, and SMMR Data. *J. of Geophys. Res.*, 113, C02S07. doi:10.1029/2007JC0043257.

Comiso, J. C., D. Cavalieri, C. Parkinson, and P. Gloersen. (1997). Passive Microwave Algorithms for Sea Ice Concentrations: A Comparison of Two Techniques. *Rem. Sens. of the Environ*., 60(3):357-384.

Comiso, J. C. 1986. Characteristics of Arctic Winter Sea Ice from Satellite Multispectral Microwave Observations. *J. Geophys. Res*., 91(C1): 975-994.

Eaton B., J. Gregory, H. Centre, B. Drach, K. Taylor, and S. Hankin. (2010). NetCDF Climate and Forecast (CF) Metadata Conventions Version 1.5. *Programs for Climate Model Diagnosis and Intercomparison*. 81 pp. http://cf-pcmdi.llnl.gov/documents/cf-conventions/1.5/cf-conventions.pdf. Accessed Sep. 2011.

Fetterer, F., M. Dorfman, B. R. Brasher, and A. Windnagel. Edge of Antarctica: Two Differing Perspectives on Where Ice and Water Mix. Poster presented at: American Meteorological Society 101st Annual Meeting, 10-15 January 2021, virtual. Retrieved from https://ams.confex.com/ams/101ANNUAL/meetingapp.cgi/Paper/381502

Fetterer, F., and N. Untersteiner. (1998). Observations of Melt Ponds on Arctic Sea Ice. *J. Geophys. Res*., 103(C11): 24,821-24,835.

Ivanova, N., Pedersen, L. T., Tonboe, R. T., Kern, S., Heygster, G., Lavergne, T., Sørensen, A., Saldo, R., Dybkjær, G., Brucker, L., & Shokr, M. (2015). Inter-comparison and evaluation of sea ice algorithms: towards further identification of challenges and optimal approach using passive microwave observations. *The Cryosphere*, 9: 1797–1817. doi: 10.5194/tc-9-1797-2015.

Kern, S., Rösel, A., Pedersen, L. T., Ivanova, N., Saldo, R., & Tonboe, R. T. (2016). The impact of melt ponds on summertime microwave brightness temperatures and sea-ice concentrations. *The Cryosphere*, 10: 2217–2239. doi: 10.5194/tc-10-2217-2016.

Kern, S., Lavergne, T., Notz, D., Pedersen, L. T., Tonboe, R. T., Saldo, R., & Sørensen, A. M. (2019). Satellite passive microwave sea-ice concentration data set intercomparison: closed ice and ship-based observations. *The Cryosphere*, 13: 3261–3307. doi: 10.5194/tc-13-3261-2019.

Kern, S., Lavergne, T., Notz, D., Pedersen, L. T., & Tonboe, R. (2020). Satellite passive microwave sea-ice concentration data set inter-comparison for Arctic summer conditions. *The Cryosphere*, 14: 2469–2493. doi: 10.5194/tc-14-2469-2020.

Kwok, R. (2002). Sea Ice Concentration Estimates from Satellite Passive Microwave Radiometry and Openings from SAR Ice Motion. *Geophys. Res. Lett*., 29(9): 1311. doi:10.1029/2002GL014787.

Meier, W. N., Stewart, J. S., Windnagel, A., and Fetterer, F. M. (2022). Comparison of Hemispheric and Regional Sea Ice Extent and Area Trends from NOAA and NASA Passive Microwave-Derived Climate Records. *Remote Sens.* 14(3), 619. doi: https://doi.org/10.3390/rs14030619.

Meier, W. N., A. Windnagel, S. Stewart. (2021). CDR Climate Algorithm and Theoretical Basis Document: Sea Ice Concentration, Rev 9. NOAA NCEI CDR Program.

Meier, W. N., G. Peng, D. J. Scott, and M. H. Savoie. (2014). Verification of a new NOAA/NSIDC passive microwave sea-ice concentration climate record. *Polar Research* 33. doi: 10.3402/polar.v33.21004.

Meier, W. N. and the National Center for Atmospheric Research (NCAR) Staff (Eds). (2014). "The Climate Data Guide: Sea Ice Concentration: NOAA/NSIDC Climate Data Record." Retrieved 04 June 2015 from https://climatedataguide.ucar.edu/climate-data/sea-ice-concentration-noaansidc-climate-data-record.

Meier, W. N., and S. J. S. Khalsa. (2011). Intersensor Calibration between F13 SSM/I and F17 SSMIS Near-Real-Time Sea Ice Estimates. *Geoscience and Remote Sensing* 49(9): 3343-3349.

Meier, W. N. (2005). Comparison of Passive Microwave Ice Concentration Algorithm Retrievals with AVHRR Imagery in Arctic Peripheral Seas. IEEE Trans. *Geosci. Remote Sens*., 43(6): 1324-1337.

Partington, K., T. Flynn, D. Lamb, C. Bertoia, and K. Dedrick. (2003). Late Twentieth Century Northern Hemisphere Sea-Ice Record from U.S. National Ice Center Ice Charts. *J. Geophys. Res*. 108(C11): 3343. doi:10.1029/2002JC001623.

Peng, G., A. Arguez, W. N. Meier, F. Vamborg, J. Crouch, P. Jones. (2019). Sea Ice Climate Normals for Seasonal Ice Monitoring of Arctic and Sub-Regions. *Data* 4(3) 122. https://doi.org/10.3390/data4030122.

Peng, G., W. N. Meier, D. J. Scott, and M. H. Savoie. (2013). A long-term and reproducible passive microwave sea ice concentration data record for climate studies and monitoring. *Earth Syst. Sci. Data* 5: 311-318. doi: 10.5194/essd-5-311-2013.

Steffen, K., J. Key, D. J. Cavalieri, J. Comiso, P. Gloersen, K. St. Germain, and I. Rubinstein. (1992). The Estimation of Geophysical Parameters using Passive Microwave Algorithms, in "Microwave Remote Sensing of Sea Ice." F.D. Carsey, ed., *American Geophysical Union Monograph* 68, Washington, DC:201-231.

National Research Council of the National Academies. (2004). Climate Data Records from Environmental Satellites: Interim Report. National Academies Press, Washington, D.C., 150 pp.

Windnagel, A., Meier, W., Stewart, S., Fetterer, F., & Stafford, T. (2021). NOAA/NSIDC Climate Data Record of Passive Microwave Sea Ice Concentration Version 4 Analysis. *NSIDC Special Report 20*. Boulder CO, USA: National Snow and Ice Data Center.

9 DOCUMENT INFORMATION

9.1 Author

A. Windnagel

9.2 Publication Date

July 2011

9.3 Revision History

August 2024: A. Windnagel updated the document to describe the addition of the STAC catalog and added more information on how the temporal interpolation is performed.

May 2021: A. Windnagel updated the document to reflect changes with the release of Version 4 Revision 0.

October 2018: A. Windnagel updated the version history section to note the release of the 2017 data and added a technical note about the Bootstrap data to the Input Data section.

December 2017: A. Windnagel updated the version history section to note the changes and updates to Version 3 Revision 1.

August 2017: A. Windnagel updated the document to represent Version 3 Revision 0 changes and updates.

May 2016: A. Windnagel updated the document with the Variables at a Glance tables and made other minor edits.

August 2015: A. Windnagel updated the flow chart diagrams and the version history to reflect the new modularization done to the code.

June 2015: A. Windnagel added the Differences in the NOAA/NSIDC Concentration CDR Variables and the Merged GSFC-Produced Concentration Variables section to clarify which variable to use.

July 2014: A. Windnagel updated the temporal coverage to reflect the new 2013 data that was processed.

March 2013: A. Windnagel updated the document to describe the new Version 2 Revision 00 of these data. Added new processing flowcharts, new melt variable description, and updated the description of the melt detection QA flag. Also added that the temporal coverage now spans through 2012.

May 2012: A. Windnagel added the monthly file information and put the document into the new guide doc style.